A polarimetric study of optical anisotropy in the rare-earth cuprates R_2CuO_4

1994 J. Phys.: Condens. Matter 6 4795

(http://iopscience.iop.org/0953-8984/6/25/017)

J. Phys.: Condens. Matter 6 (1994) 4795–4805. Printed in the UK

A polarimetric study of optical anisotropy in the rare-earth cuprates R_2CuO_4

B B Krichevtsov†, R V Pisarev†, A Burau‡, H-J Weber‡, S N Barilo§ and D I Zhigunov§

† Ioffe Physico-Technical Institute of the Russian Academy of Sciences, 194021 St Petersburg, Russia

‡ Physics Department, Dortmund University, 44221 Dortmund, Germany

§ Institute of Solid State Physics and Semiconductors of the Academy of Sciences, 220726 Minsk, Belorussia

Received 25 October 1993, in final form 7 April 1994

Abstract. The optical dielectric function of the *ac* plane of rare-earth cuprate (R_2CuO_4) single crystals in the energy range 1.2–2.7 eV is measured in reflection by a polarimetric method. The dispersion of optical anisotropy in insulating samples is described by two oscillators separated by 0.4 eV. Conducting samples can be identified by a Drude-like contribution. The sensitivity of the applied method allows us to test surface quality and the influence of electric transport properties on optical anisotropy.

1. Introduction

The dominant role of CuO_2 layers in high-temperature superconductors has led to a number of optical experiments [1]. Of special interest are anisotropic properties that can be directly attached to the physics of the CuO_2 planes. A comparison of results obtained on superconductors and related non-superconducting materials containing CuO_2 planes is of prime importance. In the optical region 1–3 eV the rare-earth compounds R_2CuO_4 exhibit an optical transition that is known to be strongly polarized in the *ab* plane (see, e.g., [2]). The exact resonance energy depends on the coordination of the copper ions. This resonance has already been examined in reflection experiments by several authors [1–11]. In these experiments the spectral dependence of the reflectance is used to determine the complex dielectric function $\epsilon(\omega)$ via a Kramers–Kronig transformation. The accuracy of this procedure depends on the spectral range available. In the case of conducting $YBa_2Cu_3O_{7-x}$ it was argued that cut-off effects led to unreliable optical dielectric constants [12].

In this work we demonstrate an alternative approach to analyse the optical properties of a selection of R_2CuO_4 (R = Nd, Sm, Eu, Gd/Ce, La) samples. Most samples are insulating, some are doped. The presented method is based on the direct determination of the optical anisotropy. This is done in reflection with normal incidence. The advantage of this procedure is a direct comparison of optical properties in two orthogonal polarizations. Therefore, the sensitivity concerning anisotropic properties of features present in both polarizations is intrinsically larger than in common ellipsometric and photometric measurements, where two polarizations have to be recorded sequentially. In contrast to photometric experiments no Kramers–Kronig transformation is needed for the determination of optical constants. One reason that polarimetry is scarcely used in reflection is the

0953-8984/94/254795+11$19.50

simple fact that materials which are not transparent in the visible spectral range (metals and semiconductors) are usually isotropic. Moreover, the polarimetric method suffers from a principal disadvantage: because different contributions to anisotropy may exhibit opposite signs, it is difficult or even impossible to analyse the dispersion of optical quantities. Both reasons for avoiding polarimetric measurements are absent from cuprate superconductors and from the related compounds R_2CuO_4 due to the two-dimensionality of the CuO_2 planes. Therefore, these materials are by nature favoured for a study of optical anisotropy.

The attractive feature of polarimetric measurements is their high sensitivity, especially in studying the impact of external forces on optical quantities. For many potential applications of the method a laser beam is needed to achieve maximum sensitivity. As such measurements can be rather time consuming the idea to investigate cuprates systematically by polarimetric methods is only reasonable if results obtained at discrete wavelengths can be analysed reliably. This point is studied in the present work. A second intention was a characterization of the state of doping of a sample by its optical anisotropy. In addition to anisotropy measurements an ellipsometric determination of the mean optical constants at one photon energy has been performed in order to support the evaluation of anisotropy data.

2. Experimental details

Light reflected at the surface of an anisotropic crystal changes its polarization state. Neglecting depolarization, these changes can be described by a 2×2-matrix formalism [13, 14]. The crystal matrix $\hat{R}$ describing normal reflection from the surface of an orthorhombic crystal can be reduced to the form

$$\hat{R} = R \begin{pmatrix} 1 + \rho \cos 2\xi & \rho \sin 2\xi \\ \rho \sin 2\xi & 1 - \rho \cos 2\xi \end{pmatrix} \tag{1}$$

where $\rho = \rho' + i\rho''$ is the complex linear anisotropy normalized to the mean reflection coefficient R. The optical properties are defined by the projection of the optical indicatrix on the reflecting surface. The angle ξ denotes the azimuthal orientation of this projection with respect to the laboratory system. Since in our experiments we examine the ac plane of tetragonal crystals ρ is given by

$$\rho = \frac{n_c - n_a}{n_a n_c - 1} \tag{2}$$

where $n = n' + in''$ is the complex index of refraction. The subscripts refer to the crystal axes.

Optical set-ups for the determination of real and imaginary parts of ρ are sketched in figures 1(a) and 1(b), respectively. The birefringent wedge BW serves as both polarizer and analyser. It is cut from an optically uniaxial crystal (KH_2PO_4) with its optical axis normal to the plane of incidence. Thus, ordinary and extraordinary beams are separated spatially by different angles of deflection.

If in figure 1(a) the incident linear polarization is parallel to one of the crystal axes, the polarization will remain unchanged under reflection and the reflected light will be completely transmitted back to the light source. Rotating the sample by an angle ξ changes the polarization of the reflected light and results in a component orthogonal to the original polarization. This component is deflected onto the photodetector by the wedge. The inserted

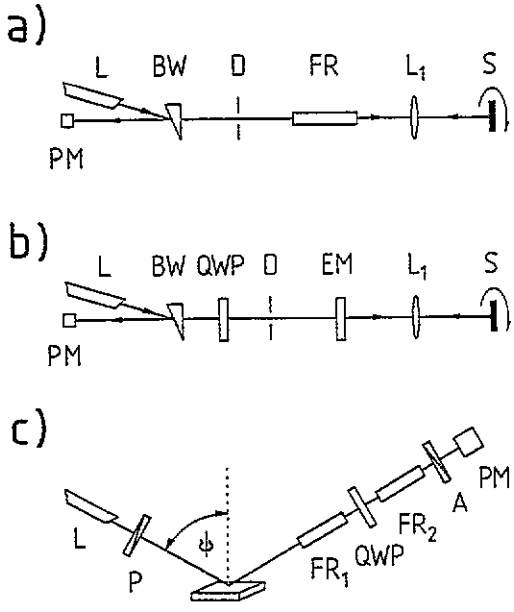

Figure 1. Experimental set-ups used to determine (*a*) ρ', (*b*) ρ'' and (*c*) the mean refractive indices. A: analyser; BW: birefringent wedge; EM: electro-optical modulator; FR: Faraday rotator; L: laser; L_1: lens; P: polarizer; PM: photo-multiplier; QWP: quarter-wave plate; S: sample.

Faraday rotator FR, driven with alternating current, produces an intensity modulation at the photodetector that is recorded by a lock-in technique. The signals at the first and second harmonics of the modulation frequency ν_{FR} are

$$I(\nu_{FR}) = 2I_0\rho'\theta_{FR}\sin 2\xi \tag{3}$$

$$I(2\nu_{FR}) = I_0\theta_{FR}^2 \tag{4}$$

where θ_{FR} is the amplitude of rotation induced by the Faraday rotator and I_0 is the intensity of light reflected by the sample. Equations (3) and (4) are valid for small amplitudes θ_{FR} only. The ratio of these two signals

$$\frac{I(\nu_{FR})}{I(2\nu_{FR})} = 2\frac{\rho'\sin 2\xi}{\theta_{FR}} \tag{5}$$

recorded as a function of the sample orientation ξ immediately yields the real part of ρ.

For measuring the imaginary part ρ'' the Faraday rotator is replaced by a quarter-wave plate and an electro-optical modulator (cf. figure 1(*b*)). The signal at the frequency of the electro-optical modulator is given by

$$I(\nu_{EM}) = I_0[8\alpha(1+\rho'') - 4\rho''\sin 2\xi]\epsilon_{EM} \tag{6}$$

where $\alpha \ll 1$ is the azimuth of the quarter-wave plate; ϵ_{EM} is the amplitude of ellipticity induced by the modulator. Since the signal of the electro-optical modulator vanishes at

$$\alpha_0 = \frac{\rho''\sin 2\xi}{2(1+\rho'')} \tag{7}$$

the quantity ρ'' is determined by recording α_0 as a function of the sample azimuth ξ.

The measurements are performed by rotating the sample in steps of 2 mrad around the position of minimum static intensity $\xi = 0$. This yields the maximum signal-to-noise ratio. Note that, although shown separately, the above measurements of ρ' and ρ'' can be performed simultaneously. An Ar^+ laser (2.4–2.7 eV), an He–Ne laser (1.96 eV) and a Ti:Al_2O_3 laser (1.2–1.6 eV) are used as light sources.

To determine the complex refractive indices of our samples we use a traditional ellipsometric set-up [13], which is sketched in figure 1(*c*). The sample S is aligned with two of its principal axes in the plane of incidence. Measurements are performed at the He–Ne energy of 1.96 eV on all {010} and {001} faces present in the samples. The azimuth of the incident linear polarized light is defined by the orientation of the polarizer P. The polarization of the reflected light is determined by the azimuthal orientations of the quarter-wave plate QWP and analyser A which yield the minimum intensity at the detector PM. In this orientation of the two optical elements the intensity signals of the two AC-driven Faraday rotators vanish so that the azimuth and ellipticity of the reflected light can be determined with high sensitivity.

The change of polarization during reflection is simply described by a 2×2 matrix $\hat{R}$ containing the Fresnel coefficients:

$$\hat{R} = \begin{pmatrix} -\dfrac{\sin(\psi - \phi)}{\sin(\psi + \phi)} & 0 \\ 0 & \dfrac{\tan(\psi - \phi)}{\tan(\psi + \phi)} \end{pmatrix}. \tag{8}$$

Here ψ is the angle of incidence and ϕ is the (complex) angle of deflection. The polarization (1; 0) is taken to be normal to the plane of incidence. The measurements are performed with different incident polarizations to be independent of, for example, spurious birefringences in the set-up, and with varying angle of incidence ψ. The complex refractive index is then evaluated using standard ellipsometric equations [15]. To increase accuracy, equation (2) and the quantity ρ determined in reflection are used to fix the optical anisotropy $n_c - n_a$ so that only the ordinary refractive index n_a is fitted. The resulting values of n_a and n_c are listed in table 1.

Table 1. Characteristic data of the R_2CuO_4 samples: specific resistance ρ_{ab}, temperature of tetragonal-to-orthorhombic phase transition T_{th}, Néel temperature T_N and refractive index $n = n' + in''$ for a and c axes at 1.96 eV photon energy.

X=CuO_4	La_2X (1)	La_2X (2)	Nd_2X	Sm_2X	Eu_2X	$Gd_{1.93}Ce_{0.07}X$
ρ_{ab} ($10^3\Omega$ cm)	1.4	0.09	17	2.9	4.5	—
T_{th} (K)	522	512	—	—	—	—
T_N (K)	—	281	252	265	250	—
n'_a	2.52(4)	2.23(4)	1.90(3)	2.04(4)	2.05(7)	1.93(3)
n''_a	0.55(4)	0.61(4)	1.02(3)	0.59(12)	0.56(6)	0.43(12)
n'_c	2.05(4)	2.86(4)	2.45(3)	1.90(4)	1.94(7)	1.97(3)
n''_c	0.33(4)	0.16(4)	0.89(3)	0.08(12)	0.04(6)	0.19(12)

3. Samples

The examined single crystals of the R_2CuO_4 family were grown by a flux growth method described elsewhere [16, 17]. This family is usually classified by the coordination

of the copper atoms. Our experiments are performed on the '*T*-phase' La_2CuO_4 (octahedral coordination) and on '*T'*-phase' samples Nd_2CuO_4, Sm_2CuO_4, Eu_2CuO_4 and $Gd_{1.93}Ce_{0.07}CuO_4$ (square coordination). The La_2CuO_4 and Nd_2CuO_4 samples are bar shaped with polished *ab* and *ac* faces. Sm_2CuO_4, Eu_2CuO_4 and $Gd_{1.93}Ce_{0.07}CuO_4$ samples are thin plates of about $1\times5\times5$ mm^3. In both La_2CuO_4 samples a tetragonal-to-orthorhombic transition was observed in preliminary experiments by measuring the rotation of linearly polarized light in reflection. Sm_2CuO_4 and Eu_2CuO_4 samples were previously studied by Gukasov and co-workers [18]. Specific resistances in the *ab* plane ρ_{ab}, transition temperatures of the tetragonal-to-orthorhombic transition T_{th} and Néel temperatures T_N are given in table 1.

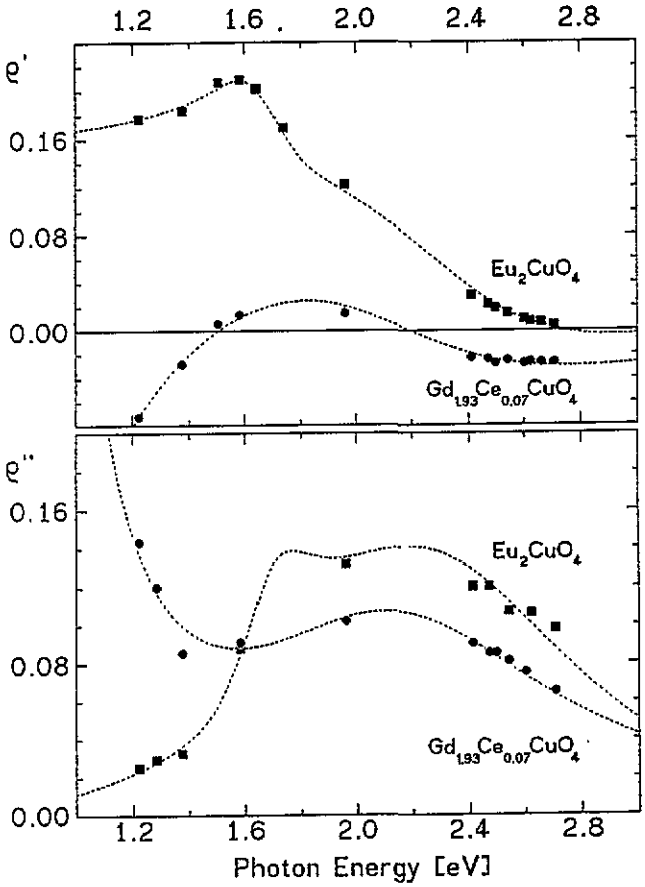

Figure 2. Real and imaginary parts of the anisotropy parameter $\rho = \rho' + i\rho''$ of Eu_2CuO_4 (■) and $Gd_{1.93}Ce_{0.07}CuO_4$ (•). Here and in figures 3–5 curves represent results of least-squares fits.

4. Results and discussion

The dependences on photon energy of the real and imaginary parts of the anisotropy parameter ρ of different samples are shown in figures 2–5. The curves are the results

of least-squares fits. As is shown in figures 2 and 3 the dispersion of ρ is similar in the insulating samples Sm_2CuO_4 and Eu_2CuO_4. The S-shaped curve in ρ' and the peak-like behaviour of ρ'' is characteristic for insulating T'-phase crystals. In contrast to this, it is obvious from figure 2 that the dispersion of the conducting (due to Ce^{4+} doping) sample $Gd_{1.93}Ce_{0.07}CuO_4$ is significantly different. ρ' and ρ'' show a Drude-like behaviour at lower photon energies whereas at higher energies they follow the dispersion of the insulating samples asymptotically. The different behaviour of insulating and conducting samples requires different methods of description.

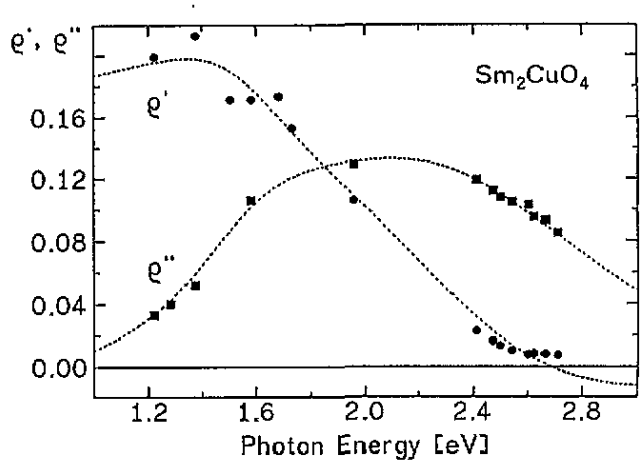

Figure 3. Spectral dependence of ρ' and ρ'' for the insulating Sm_2CuO_4 sample.

It is known that in the energy range under consideration in the non-conducting samples there are charge transfer transitions from O 2p-like to Cu 3d-like states [3, 5–11]. The fact that these transitions are strongly polarized in the ab plane allows the application of a simple model to describe the spectral dependence of the experimental data. Because of the small spectral range considered here, we assume the dielectric function of the c direction ϵ_c simply to be constant. The value of ϵ_c is fixed by the ellipsometric measurement of the mean optical constants. The resonances are supposed to contribute only to the dielectric function of the a direction:

$$\epsilon_a(\omega) = \epsilon_{\infty;a} + \sum_j \frac{f_j}{\omega_j^2 - \omega^2 - i\omega\gamma_j}. \tag{9}$$

Here, ω_j are the resonance frequencies of the oscillators describing the transitions; f_j and γ_j measure oscillator strengths and damping, respectively. The total number of oscillators is restricted due to the limited spectral range of our experiments. The attempt to approximate the dispersion of ρ in a least-squares fit with only one oscillator leads to resonance energies in the range 1.8–1.9 eV for Sm_2CuO_4 and Eu_2CuO_4, whereas under the assumption of two oscillators polarized in the ab plane we are able to reduce the residual sum-of-squares by about one order of magnitude. In this case the T'-phase samples exhibit one resonance at 1.6 eV and a second one at about 2.0 eV. The need for two oscillators also follows from a comparison of our data with results from photometry. In reflectivity a rather sharp peak is always observed [6, 10]. This peak is accompanied by some broadening at the high-energy tail. Tokura and co-workers [5] interpreted this broadening as a side band. Using

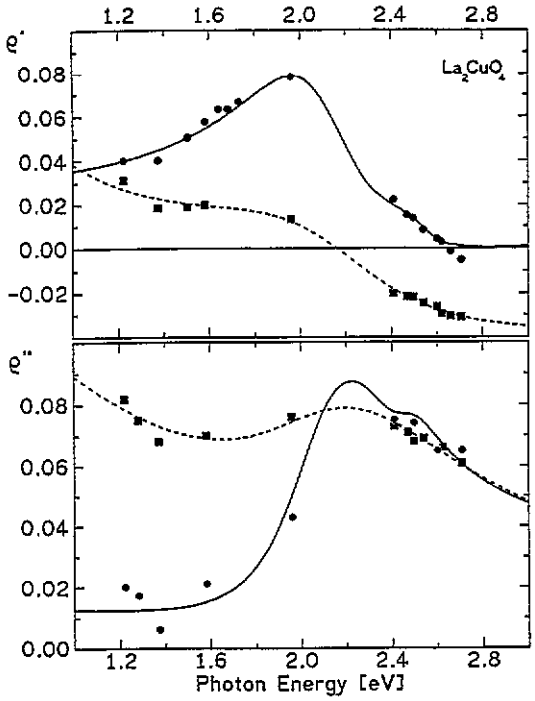

Figure 4. Dispersion of ρ' (above) and ρ'' (below) of the less conducting La_2CuO_4 (1) (•) and the more conducting La_2CuO_4 (2) (■).

the parameters obtained from the least-squares fit of our data reflectivity can be calculated. The sharp peak and the side band are well reproduced only if we take into account the results of a two-oscillator fit. In figure 6 the need for two oscillators is demonstrated in a different way. The position of the low-lying resonances obtained from our measurements is compared to the ϵ'' peaks determined by photometry [10]. Only the assumption of two resonances leads to an agreement between the two methods. The slight shift in the 1.6 eV resonance of the T'-phase crystals is correlated with the Cu–O bond length [10].

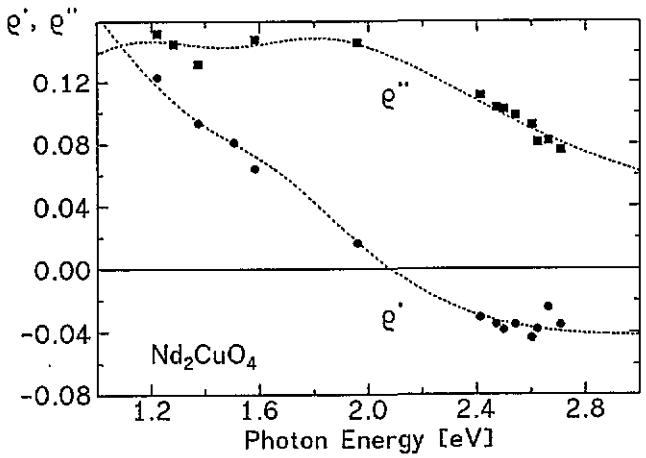

Figure 5. Spectral behaviour of ρ' and ρ'' of the insulating Nd_2CuO_4 sample.

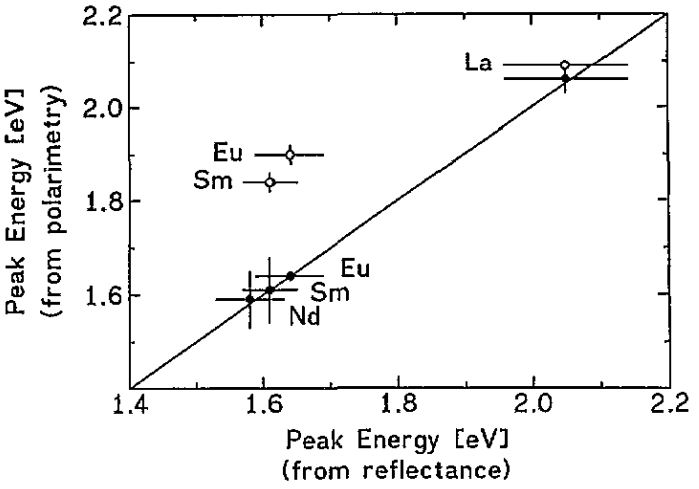

Figure 6. Peak energies of the 1.6 eV resonance (T' phase) and the 2.0 eV resonance (T phase) by Arima and co-workers [10] compared with results obtained by our polarimetric measurements assuming one (○) and two (●) oscillators.

In the conducting $Gd_{1.93}Ce_{0.07}CuO_4$ the presence of charge carriers has to be taken into account by adding a Drude-like term to the model for the dielectric function. We attribute the Drude contribution to the *ab* plane only. This is reasonable because in the optical region the Drude term shows only a moderate dispersion and because in our optical experiments we detect differences mainly between the *ab* plane and the *c* direction. To reduce the total number of fit parameters to a reasonable value we add only one oscillator in this case. The model for ϵ_a is therefore

$$\epsilon_a(\omega) = \epsilon_{\infty;a}\left(1 - \frac{\omega_p^2}{\omega^2 + i\omega/\tau}\right) + \frac{f}{\omega_0^2 - \omega^2 - i\omega\gamma} \tag{10}$$

where ω_p is the plasma frequency and τ describes the damping of charge carrier motion. From figure 2 it is obvious that this is sufficient to describe the dispersion of ρ. In figure 7 we plot the contribution of the oscillators to the imaginary part of $\epsilon(\omega)$ resulting from the fits of Eu_2CuO_4 and $Gd_{1.93}Ce_{0.07}CuO_4$ separately. The direct comparison shows that in the conducting sample the 1.6 eV resonance disappears, whereas it is obvious from the position and shape of the curve that the 2.1 eV resonance survives.

The spectral behaviour of ρ' and ρ'' allows us to draw additional conclusions about the properties and quality of the samples. From a comparison of the two La_2CuO_4 samples we find significant differences. Figure 4 shows the spectral dependence of ρ' and ρ'' for the two samples. Sample 1 exhibits the usual dispersion of an insulating sample. Since La_2CuO_4 is a T-phase crystal the resonances are shifted towards higher photon energies by about 0.5 eV. The second La_2CuO_4 sample shows an intermediate behaviour between conducting and insulating samples in agreement with its higher DC conductivity (cf. table 1): a stronger anisotropy at the lower photon energies and a more monotonic than oscillatory dependence. Therefore, we include a Drude term in the ϵ_a model.

In all the above cases we find our optical measurements to be in agreement with the electrical transport properties determined independently. This is not the case in the Nd_2CuO_4 sample. From table 1 we find that this crystal shows a rather high specific resistance. On the

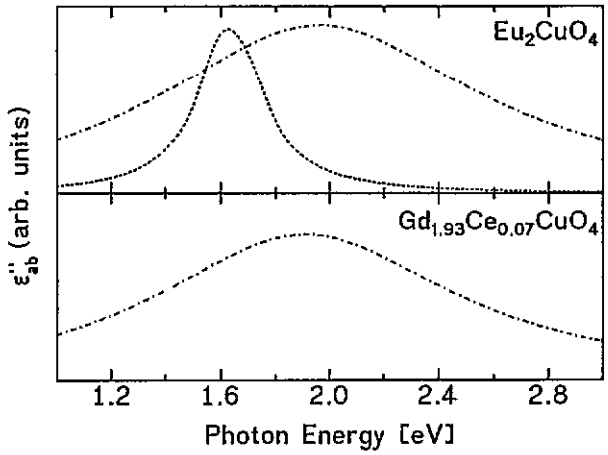

Figure 7. Contribution of the fitted oscillators to the imaginary part of the dielectric function for the insulating Eu_2CuO_4 and the conducting $Gd_{1.93}Ce_{0.07}CuO_4$.

other hand, figure 5 shows that the dispersion of ρ' and ρ'' is of intermediate type, like that of La_2CuO_4 sample 2. Since the DC conductivity mainly tests the bulk properties, whereas the results of optical reflection experiments depend sensitively on the surface quality, we attribute the modified dispersion of ρ' and ρ'' to the presence of a thin conducting surface layer that may have been formed during several temperature cycles between 80 K and 650 K in previous experiments.

In the case of the $Gd_{1.93}Ce_{0.07}CuO_4$ sample the Drude contribution to the dielectric function originates from the Ce^{4+} doping. The plasma energy $\hbar\omega = 0.94(4)$ eV resulting from the least-squares fit can therefore be compared with that of similarly doped rare-earth cuprates. Hirochi and co-workers [19] report a plasma energy of the similar T'-phase $Nd_{2-x}Ce_xCuO_4$ of 1.03–1.07 eV depending on x. This supports the reliability of our method.

Table 2. Resonance energies of the oscillators identified by a least-squares fit. In the samples marked with * a second oscillator was not included in the model for technical reasons.

	Phase	$\hbar\omega_1$ (eV)	$\hbar\omega_2$ (eV)	$\hbar\Delta\omega$ (eV)
Nd_2CuO_4	T'	1.59(6)	*	
Sm_2CuO_4	T'	1.61(7)	2.28(47)	0.67(48)
Eu_2CuO_4	T'	1.64(1)	2.08(4)	0.44(4)
$Gd_{1.93}Ce_{0.07}CuO_4$	T'	*	2.02(2)	
La_2CuO_4 (1)	T	2.06(2)	2.49(5)	0.43(5)
La_2CuO_4 (2)	T	2.13(4)	*	

In table 2 we list all resonances that could be identified. In all samples where a second oscillator can be established by the least-squares fit we find this second transition about 0.4 eV above the 1.6 eV (T'-phase) and the 2.1 eV (T-phase) resonance. Our results show that fit parameters which are a measure of oscillator strength depend crucially on the state of the sample. They are most reliable for the Eu_2CuO_4 sample. In this case $\hbar^2 f_1 = 1.0(3)\,\mathrm{eV}^2$, $\hbar\gamma_1 = 0.28(6)$ eV and $\hbar^2 f_2 = 6.5(1.2)\,\mathrm{eV}^2$, $\hbar\gamma_2 = 1.4(2)$ eV for the 1.6 eV and the 2.0 eV resonances, respectively. The same tendency, $\gamma_1 < \gamma_2$ and $f_1 < f_2$, is found in the second insulating T'-phase sample Sm_2CuO_4. In contrast to this the insulating T-phase La_2CuO_4

shows $f_1 \gg f_2$. Therefore, the second oscillator in La_2CuO_4 is not so well established as in the T'-phase crystals. The band structure of T- and T'-phase crystals [20] is rather complex and offers several possibilities for an assignment of the second transition. For a definite assignment additional features of this band need to be known.

5. Conclusion

In this paper we present the first experimental data of a polarimetric study of the optical anisotropy in R_2CuO_4 crystals. In contrast to conventional reflection measurements (ellipsometry, photometry) polarimetry is a method that probes directly the anisotropy of a sample. As a difference of two optical quantities is determined one can expect that the influence of surface contamination and surface roughness is suppressed. Even though only discrete photon energies are used, our results show that the dispersion of optical parameters can be determined reliably. In particular, we have shown that optical anisotropy depends sensitively on doping. Therefore, the polarimetric method can be a useful tool for studying the optical parameters of cuprates as a function of temperature, stoichiometry and different annealing procedures.

In insulating R_2CuO_4 we observe two transitions. The resonance energy of the low-lying transition is near 1.6 eV in T'-phase crystals (depending in detail on R) and at 2.1 eV in the T-phase crystal La_2CuO_4. These values and the disappearance of the transition on doping are consistent with photometric measurements reported previously [9]. The second transition is clearly revealed 0.4 eV above the first one in insulating T'-phase crystals. Two aspects suggest that this transition is important for an understanding of the electronic properties of these materials. Firstly, it survives doping in contrast to the nearest transition at 1.6 eV [9]. Secondly, its oscillator strength is larger than that of the 1.6 eV transition.

Acknowledgments

We would like to thank S A Kizhaev for magnetic measurements on the La_2CuO_4 samples. Fruitful discussions with J Blechschmidt, A L Shelankov and V V Pavlov are appreciated. This work was supported by the Russian Programme on High-Temperature Superconductors, project No 92096, by the Deutsche Forschungsgemeinschaft and by the Soros Foundation Grant awarded by the American Physical Society.

References

[1] Timusk T and Tanner D B 1989 *Physical Properties of High Temperature Superconductors* vol 1, ed D M Ginsberg (Singapore: World Scientific) p 339
[2] Falck J P, Levy A, Kastner M A and Birgenau R J 1992 *Phys. Rev. Lett.* **69** 1109
[3] Tajima S, Ishii H, Nakahashi T, Takagi T, Uchida S, Seki M, Suga S, Hidaka Y and Suzuki M 1989 *J. Opt. Soc. Am.* B **6** 475
[4] Eklund P C, Rao A M, Lehmann G W, Doll G L, Dresselhaus M S, Picone P J, Gabbe D R, Jenssen H P and Dresselhaus G 1989 *J. Opt. Soc. Am.* B **6** 389
[5] Tokura Y, Takagi H, Arima T, Koshihara S, Ido T, Ishibashi S and Uchida S 1989 *Physica* C **162–164** 1231
[6] Tokura Y, Koshihara S, Arima T, Takagi H, Ishibashi S, Ido T and Uchida S 1990 *Phys. Rev.* B **41** 11 657
[7] Cooper S L, Thomas G A, Orenstein J, Rapkine D H, Millis A J, Cheong S-W and Cooper A S 1990 *Phys. Rev.* B **41** 11 605
[8] Cooper S L, Thomas G A, Mills A J, Sulewski P E, Orenstein J, Rapkine J H, Cheong S-W and Trevor P L 1990 *Phys. Rev.* B **42** 10 785

[9] Uchida S, Ido T, Takagi H, Arima T, Tokura Y and Tajima S 1991 *Phys. Rev.* B **43** 7942
[10] Arima T, Kikuchi K, Koshihara S, Tokura Y, Ido T and Uchida S 1991 *Phys. Rev.* B **44** 917
[11] Thomas G A, Rapkin D H, Cooper S L, Cheong S-W, Cooper A S, Schneemeyer L F and Wascak J V 1992 *Phys. Rev.* B **45** 2474
[12] Bozovic I 1990 *Phys. Rev.* B **42** 1969
[13] Azzam R M A and Bashara N M 1977 *Ellipsometry and Polarized Light* (Amsterdam: North-Holland)
[14] Kliger D S, Lewis J W and Randall C E 1990 *Polarized Light in Optics and Spectroscopy* (New York: Academic)
[15] Born M and Wolf E 1965 *Principles of Optics* (Oxford: Pergamon)
[16] Barilo S N, Ges A P, Guretskiy S A *et al* 1989 *Sverhprov.: Fiz. Chem. Techn.* **2** 138
[17] Barilo S N, Zhigunov Z I, Ges A P *et al* 1989 *Adv. Creog. Eng.* A **36** 627
[18] Gukasov A G, Kokovin S Y, Plakhty V P, Zobkalo I A, Barilo S N and Zhigunov D I 1992 *Physica* B **180–181** 455
[19] Hirochi K, Hayashi S, Adachi H, Mitsuyu T, Hirao T, Setsune K and Wasa K 1989 *Physica* C **160** 273
[20] Ovchinnicov S G 1992 *Sov. Phys.–JETP* **75** 67